

VORTEX FILAMENT IN THREE-MANIFOLD AND THE DUISTERMAAT-HECKMAN FORMULA *

Yukinori Yasui [†]

*Department of Physics, Osaka City University,
Sugimoto, Sumiyoshi-Ku, Osaka 558, Japan*

Waichi Ogura [‡]

*Department of Physic, Osaka University,
Machikaneyama, Toyonaka-Shi, Osaka 560, Japan*

September 6, 2018

Abstract

Symplectic geometry of the vortex filament in a curved three-manifold is investigated. There appears an infinite sequence of constants of motion in involution in the case of constant curvature. The Duistermaat-Heckman formula is examined perturbatively for the classical partition function in our model and verified up to the 3-loop order.

*Keywords: symplectic geometry, integrable models, Hasimoto map, WKB exactness, the Duistermaat-Heckman Formula, loop space, zeta-function regularization.

[†]E-mail: h1879@ocugw.cc.osaka-cu.ac.jp

[‡]E-mail: ogura@funpth.phys.sci.osaka-u.ac.jp

1 Introduction

Kinematics of a very thin vortex tube in three-dimensional fluid may be described by the filament equation in the local induction approximation [1, 2]. It is formulated as

$$\frac{\partial \gamma}{\partial t} = \frac{\partial \gamma}{\partial s} \times \frac{\partial^2 \gamma}{\partial s^2}, \quad (1)$$

where $\gamma = \gamma(t, s)$ denotes the position of the vortex filament in \mathbb{R}^3 with t and s being the time and the arc-length parameter respectively.

Hasimoto [3] introduced a map $h : \gamma \mapsto \psi = \kappa \exp[i \int^s \tau(u) du]$, in order to transform the filament equation into the nonlinear Schrödinger (NLS) equation for ψ . Here κ and τ respectively denote the curvature and the torsion along γ . Since the integrability of the NLS equation was well known, the filament equation was naturally expected to be integrable. Mardson and Weinstein [4] first described the filament equation as a Hamiltonian equation with the Hamiltonian simply being the length $\ell[\gamma]$ of the vortex filament. Later Langer and Perline [5] used this Hamiltonian structure to prove the existence of an infinite sequence of constants of motion in involution, and studied the evolution of the vortex filaments in connection with the solitons in the NLS equation.

With this concern in mind, we have investigated the filament equation in a curved three-manifold M . Although Langer and Perline have limited M to \mathbb{R}^3 , we find an analogous integrable hierarchy in the case of constant curvature. We further study the classical partition function for the vortex filaments

$$Z(\beta) = \int_{\Gamma} e^{-\beta \ell[\gamma]} \mathcal{D}\gamma. \quad (2)$$

It is not clear if the Duistermaat-Heckman formula [6] applies to this case, because our phase space Γ is neither finite dimensional nor compact, and furthermore because the Hamiltonian flow may not be periodic. But the perturbative calculation in our mode reveals that the loop corrections to the formula vanish up to the 3-loop.

2 Integrability

We begin this section by describing a symplectic structure for the vortex filament in a three-manifold M equipped with a Riemann metric g . Everything is considered in the smooth category for simplicity. Let Γ be the space of vortex filaments with fixed end points p and q ; Γ is the quotient space of $\{\gamma : [0, 1] \rightarrow M \mid \gamma(0) = p, \gamma(1) = q\}$ with the reparametrization of γ . Hereafter γ denotes the representative for which the parameter $x \in [0, 1]$ is a multiple of the arc-length s , namely

$$\frac{ds}{dx} = \left\| \frac{d\gamma}{dx} \right\| = \sqrt{\left(\frac{d\gamma}{dx}, \frac{d\gamma}{dx} \right)} \quad (3)$$

is independent of x . Here (\cdot, \cdot) denotes the inner product on the tangent space $T_{\gamma(x)}M$. One can identify the tangent space $T_\gamma\Gamma$ with the subspace of $\Gamma(\gamma^*TM)$, and expand $X \in \Gamma(\gamma^*TM)$ in the Frenet-Serret frame along γ such that

$$X = f \mathbf{T} + g \mathbf{N} + h \mathbf{B}, \quad (4)$$

where \mathbf{T} is the unit tangent vector to γ , \mathbf{N} is the unit normal vector and \mathbf{B} is the unit binormal vector. Let $\ell[\gamma]$ be the length of γ , so that $s = \ell[\gamma]x$. The Frenet-Serret equations are

$$\nabla_s \mathbf{T} = \kappa \mathbf{N}, \quad \nabla_s \mathbf{N} = -\kappa \mathbf{T} + \tau \mathbf{B}, \quad \nabla_s \mathbf{B} = -\tau \mathbf{N}, \quad (5)$$

with ∇ being the connection on γ^*TM induced by the Levi-Civita connection on TM . Let \wp be the projection from $\Gamma(\gamma^*TM)$ to $T_\gamma\Gamma$, then one can show that the tangent component of $v = \wp(X) \in T_\gamma\Gamma$ satisfies

$$\frac{d}{dx} v_{\mathbf{T}} = \ell^{-1}(\nabla_x v, \frac{d\gamma}{dx}) + \ell \kappa v_{\mathbf{N}}, \quad (6)$$

and $(\nabla_x v, d\gamma/dx)$ is a constant. Fixing this constant by the boundary conditions $X(0) = X(1) = 0$, one obtains

$$\wp(X) = v = \ell \left(\int_0^x \kappa v_{\mathbf{N}} dx - x \int_0^1 \kappa v_{\mathbf{N}} dx \right) \mathbf{T} + v_{\mathbf{N}} \mathbf{N} + v_{\mathbf{B}} \mathbf{B}. \quad (7)$$

Geometrical structures on Γ were first studied by Marsden and Weinstein [4] for the vortex filament in \mathbf{R}^3 , and generalized to the loop space for a three-manifold M by Brylinski [7]. It is straightforward to find those for the vortex filament in M .

i) Complex structure

For the tangent vector $v \in T_\gamma\Gamma$, J generates the 90-degree rotation

$$J(v) = -\wp(\mathbf{T} \times v), \quad J^2 = -1. \quad (8)$$

Choosing $(v_{\mathbf{N}}, v_{\mathbf{B}})$ as coordinates for $T_\gamma\Gamma$, we find that J corresponds to the multiplication by i for the complex function $v_{\mathbf{N}}(x) + i v_{\mathbf{B}}(x)$. Hence J induces a complex structure on Γ .

ii) Riemann structure

The Riemann structure on Γ is simply defined by

$$\langle u, v \rangle_\Gamma = \ell \int_0^1 (u_{\mathbf{N}} v_{\mathbf{N}} + u_{\mathbf{B}} v_{\mathbf{B}}) dx \quad (9)$$

for $u, v \in T_\gamma\Gamma$, and satisfies the hermitian condition

$$\langle u, v \rangle_\Gamma = \langle J(u), J(v) \rangle_\Gamma. \quad (10)$$

Note that even though $\langle \cdot, \cdot \rangle_\Gamma$ ignores the \mathbf{T} -components, it is non-degenerate.

iii) Symplectic structure

The volume form ν on M associated with the Riemann metric g provides the symplectic structure on Γ , namely

$$\omega(u, v) = \int_0^1 \nu\left(\frac{d\gamma}{dx}, u, v\right) dx. \quad (11)$$

Using the Frenet-Serret frame, one can rewrite this as

$$\omega(u, v) = \ell \int_0^1 (u_{\mathbf{N}}v_{\mathbf{B}} - u_{\mathbf{B}}v_{\mathbf{N}}) dx, \quad (12)$$

which is equivalent to the one constructed from the above two structures

$$\omega(u, v) = \langle u, J(v) \rangle_{\Gamma}. \quad (13)$$

Having set out the basic structures, we now turn to the Hamiltonian flows for the vortex filament. Let $\ell : \Gamma \mapsto \mathbb{R}$ be a smooth Hamiltonian function, then the Hamiltonian vector field X_{ℓ} has the form

$$X_{\ell} = J(\text{grad } \ell). \quad (14)$$

Choosing $i_{X_{\ell}} \omega = d\ell$ and putting $v = d\gamma_t/dt|_{t=0}$, we get

$$\begin{aligned} v \ell [\gamma] &= \frac{d}{dt} \int_0^1 \sqrt{\left(\frac{\partial \gamma_t}{\partial x}, \frac{\partial \gamma_t}{\partial x}\right)} dx \Big|_{t=0}, \\ &= \frac{1}{\ell[\gamma]} \int_0^1 \left(\nabla_x v, \frac{d\gamma}{dx}\right) dx, \\ &= -\ell[\gamma] \int_0^1 (v, \kappa \mathbf{N}) dx. \end{aligned} \quad (15)$$

$\text{grad } \ell = -\wp(\kappa \mathbf{N})$ follows, and therefore

$$X_{\ell} = \kappa \mathbf{B}. \quad (16)$$

This yields a natural generalization of the filament equation in M [8]

$$\frac{\partial \gamma}{\partial t} = \kappa \mathbf{B} = \ell^{-3} \frac{\partial \gamma}{\partial x} \times \nabla_x \frac{\partial \gamma}{\partial x}. \quad (17)$$

The evolution equations for κ and τ are the followings

$$\frac{\partial \kappa}{\partial t} = \kappa \text{Ric}(\mathbf{B}, \mathbf{N}) - \ell^{-1} \left(2\tau \frac{\partial \kappa}{\partial x} + \kappa \frac{\partial \tau}{\partial x} \right), \quad (18)$$

$$\frac{\partial \tau}{\partial t} = \tau \text{Ric}(\mathbf{T}, \mathbf{N}) + \ell^{-1} \frac{\partial}{\partial x} \left(\frac{1}{2} \kappa^2 + \ell^{-2} \kappa^{-1} \frac{\partial^2 \kappa}{\partial x^2} - \tau^2 + \rho(\mathbf{T}, \mathbf{B}) \right), \quad (19)$$

where Ric and ρ denote the Ricci tensor and the sectional curvature on M respectively. In the case of constant curvature, these equations take simpler forms

$$\frac{\partial \kappa}{\partial t} = -\ell^{-1} \left(2\tau \frac{\partial \kappa}{\partial x} + \kappa \frac{\partial \tau}{\partial x} \right), \quad (20)$$

$$\frac{\partial \tau}{\partial t} = \ell^{-1} \frac{\partial}{\partial x} \left(\frac{1}{2} \kappa^2 + \ell^{-2} \kappa^{-1} \frac{\partial^2 \kappa}{\partial x^2} - \tau^2 \right), \quad (21)$$

which turn out to be identical with the equations appeared in [3]. Hence we can get the following proposition for a three-manifold with constant curvature.

Proposition

- (a) The filament equation is transformed into the NLS equation by the Hasimoto map.
- (b) There is an infinite sequence of constants of motion.
- (c) These constants are in involution.

Proof

We assume that κ, τ and their derivatives of arbitrary order vanish at the boundaries. Then it is straightforward to prove (a) and (b) due to the evolution equations (20) and (21). Using the explicit form of the Hamiltonian vector fields X_n (see Remark (2)), we can confirm the commutativity $\omega(X_n, X_m) = 0$ for any n and m with the help of [5], and consequently prove (c).

Remarks

- (1) The constants of motion are as follows [5]:

$$\begin{aligned} I_{-2}[\gamma] &= \ell [\gamma], \quad I_{-1}[\gamma] = \ell \int_0^1 \tau dx, \\ I_n[\gamma] &= \tilde{I}_n \circ h[\gamma] \quad (n = 0, 1, 2, \dots), \end{aligned} \tag{22}$$

where h is the Hasimoto map $h[\gamma] = \kappa \exp[i\ell [\gamma] \int_0^x \tau dx]$, and \tilde{I}_n 's are the constants of motion in the NLS equation [10] given by

$$\tilde{I}_n[\psi] = \ell \int_0^1 \frac{1}{2} \bar{\psi} \tilde{J}_n(\psi, \bar{\psi}) dx, \tag{23}$$

and

$$\tilde{J}_0 = \psi, \quad \tilde{J}_{n+1} = -i \frac{d}{ds} \tilde{J}_n - \frac{1}{4} \bar{\psi} \sum_{k=1}^n \tilde{J}_{k-1} \tilde{J}_{n-k}. \tag{24}$$

- (2) We find mutually commuting Hamiltonian vector fields X_n for $I_n[\gamma]$:

$$\begin{aligned} X_{-2} &= \kappa \mathbf{B}, \quad X_{-1} = R X_{-2}, \\ X_n &= R^{n+2} X_{-2} - c R^n X_{-2} \quad (n = 0, 1, 2, \dots), \end{aligned} \tag{25}$$

where c denotes the constant curvature and R the ‘‘recursion operator’’ defined by

$$R(v) = -\ell^{-1} \wp(\mathbf{T} \times \nabla_x v) \tag{26}$$

for $v \in T_\gamma \Gamma$. R coincides with the one appeared in [5] when we restrict v to the Hamiltonian vector fields.

- (3) Langer and Perline interpreted the Hasimoto map as a Poisson map between the Poisson structure on the space of the vertex filaments and the “forth” Poisson structure on the space of the NLS fields. We have found no such correspondence in our model, because the deformation of the vortex filament also changes its length ℓ . In the case of [5], however, the vortex filament extends boundlessly, so that the arc-length parameter is simply a parameter and does not change under the deformation. A different approach to the integrability of the vortex filaments has been investigated in [9] recently.

The filament equation belongs to an infinite hierarchy of Hamiltonian systems $\{\partial\gamma/\partial t_n = X_n \mid n = -2, -1, 0, \dots\}$, and all Hamiltonian flows in this hierarchy are transformed into those in the NLS hierarchy. In fact, the differential of h yields

$$dh : X_n \longmapsto \tilde{X}_{n+4} - 2c \tilde{X}_{n+2} + c^2 \tilde{X}_n \quad (\text{mod } i\psi), \quad (27)$$

where $\tilde{X}_{-2} = \tilde{X}_{-1} = 0$, and \tilde{X}_n ($n = 0, 1, 2, \dots$) are the Hamiltonian vector fields associated with $\tilde{I}_n[\psi]$, *i.e.*, $\tilde{X}_n = -i \text{grad } \tilde{I}_n$; first two are

$$dh(X_{-2}) = i \left(\frac{d^2\psi}{ds^2} + \frac{1}{2} |\psi|^2 \psi \right), \quad (28)$$

$$dh(X_{-1}) = \frac{d^3\psi}{ds^3} + \frac{3}{2} |\psi|^2 \frac{d\psi}{ds} + 2c \frac{d\psi}{ds}. \quad (29)$$

3 Classical partition function

In this section we evaluate the classical partition function (2) with $\mathcal{D}\gamma$ being the symplectic volume form on Γ . The stationary phase method provides an asymptotic expansion for $Z(\beta)$ as $\beta \mapsto \infty$, such that

$$Z(\beta) = \sum_{\text{grad } \ell[\gamma]=0} Z_{\text{WKB}}[\gamma, \beta] \left(1 + \frac{a_1[\gamma]}{\beta} + \frac{a_2[\gamma]}{\beta^2} + \dots \right). \quad (30)$$

The exactness of the stationary phase (WKB) approximation has been of interest due to the Duistermaat-Heckman formula [6], where they have shown that if Γ is a compact symplectic manifold and ℓ is a periodic Hamiltonian with isolated critical points, WKB approximation becomes exact for (2), *i.e.*, the asymptotic expansion terminates at Z_{WKB} . In more general arguments presented in [11], the fixed points are not necessarily isolated, and it is not mandatory to consider the circle action alone according to the analogous results obtained for higher dimensional tori. For the infinite dimensional symplectic manifolds, the WKB exactness has not been proved rigorously, but a “proper” version of WKB approximation should yield a reliable result for a large class of integrable models [12, 13, 14, 15]. With this notion in mind, we present the explicit calculation of the asymptotic expansion (30). For simplicity, we will assume the followings:

- (1) M is a three-manifold with a constant curvature c , so that the filament equation is integrable in the sense of Proposition.
- (2) Two points p and q on M are not conjugate. Consequently, the Hamiltonian ℓ is a Morse function on Γ , *i.e.*, critical points are the geodesics on M connecting p and q , and further the Hessian operator H_γ at each geodesic γ is a non-degenerate Jacobi operator

$$H_\gamma = -\nabla_x \nabla_x - c \ell[\gamma]^2. \quad (31)$$

Let us first expand the Hamiltonian ℓ around a geodesic γ . As we can see in (5), the curvature along the geodesic vanishes identically, and $\xi(x) \in T_{\gamma(x)}M$ thus satisfies the condition $(\xi, \mathbb{T}) = 0$. Using an infinitesimal deformation of γ generated by the exponential map $\gamma_s(x) = \exp_{\gamma(x)}[s \ell \xi(x)]$, we can find the expansion

$$\ell[\gamma_s] = \sum_{n=0}^{\infty} \frac{s^n}{n!} \left. \frac{d^n}{ds^n} \ell[\gamma_s] \right|_{s=0}, \quad (32)$$

$$= \ell[\gamma] \sum_{n=0}^{\infty} \frac{s^{2n}}{(2n)!} \int_0^1 W_{2n}(\xi) dx. \quad (33)$$

Here the integrand W_{2n} is given by the Bell Polynomial Y_m [16], namely

$$W_{2n}(\xi) = Y_{2n}(f_1, \dots, f_{2n}; g_1(\xi), \dots, g_{2n}(\xi)), \quad (34)$$

with

$$\begin{aligned} f_m &= (-)^{m-1} \frac{(2m-3)!!}{2^m}, \\ g_2(\xi) &= 2(\nabla_x \xi, \nabla_x \xi) - 2c \ell^2(\xi, \xi), \\ g_{2m}(\xi) &= (-)^m 2^{2m-1} \{(c \ell^2)^m(\xi, \xi)^m \\ &\quad + (c \ell^2)^{m-1}(\xi, \xi)^{m-2} [(\nabla_x \xi, \xi)^2 - (\xi, \xi)(\nabla_x \xi, \nabla_x \xi)]\} \quad (m \geq 2), \\ g_{2m+1}(\xi) &= 0. \end{aligned} \quad (35)$$

First few are given by

$$\begin{aligned} W_0 &= 1, & W_2 &= f_1 g_2, \\ W_4 &= f_1 g_4 + 3 f_2 g_2^2, & W_6 &= f_1 g_6 + 15 f_2 g_4 g_2 + 15 f_3 g_2^3. \end{aligned} \quad (36)$$

Now let us evaluate the WKB partition function

$$Z_{\text{WKB}}[\gamma, \beta] = e^{-\beta \ell[\gamma]} \int \mathcal{D}\xi \exp \left[-\frac{\beta \ell[\gamma]}{2} \int_0^1 W_2(\xi) dx \right], \quad (37)$$

$$\int_0^1 W_2(\xi) dx = \langle \xi, H_\gamma(\xi) \rangle_\Gamma. \quad (38)$$

Using the zeta-function regularization technique, we can perform the infinite dimensional integral in (37), and obtain [17]

$$Z_{\text{WKB}}[\gamma, \beta] = e^{-\beta \ell[\gamma] \pm \frac{\pi}{4} i (\eta_H(0) - \zeta_H(0))} e^{\frac{1}{2} \zeta_H'(0)} (\beta \ell[\gamma])^{-\frac{1}{2} \zeta_H(0)}, \quad (39)$$

with $\eta_H(z)$ and $\zeta_H(z)$ ($z \in \mathbb{C}$) being eta and zeta functions associated with the Hessian operator H_γ respectively. Evaluating these functions for γ with the Morse index $\mu(\gamma)$, we find

$$\eta_H(0) = -1 - 2\mu(\gamma), \quad \zeta_H(0) = -1, \quad \zeta_H'(0) = 2 \ln \left| \frac{\sqrt{c} \ell[\gamma]}{2 \sin(\sqrt{c} \ell[\gamma])} \right|, \quad (40)$$

and eventually this gives us an explicit expression

$$Z_{\text{WKB}}[\gamma, \beta] = \frac{1}{2} e^{-\beta \ell[\gamma]} \sqrt{\beta \ell[\gamma]} \left| \frac{\sqrt{c} \ell[\gamma]}{\sin(\sqrt{c} \ell[\gamma])} \right| e^{\mp \frac{\pi}{2} i \mu(\gamma)}. \quad (41)$$

Since $\mu(\gamma)$ is an even integer, the last factor contains no ambiguities.

We now proceed to the higher-order calculation. It is convenient to choose an orthogonal frame $\{e_1, e_2\}$ along γ such that

$$\nabla_x e_i = 0, \quad (\mathbb{T}, e_i) = 0 \quad \text{for } i = 1, 2. \quad (42)$$

In this frame, the kernel of the Jacobi operator H_γ becomes diagonal, and both of the diagonal elements are identical to the Dirichlet Green function

$$G(x, x') = 2 \sum_{n=1}^{\infty} \frac{\sin(n\pi x) \sin(n\pi x')}{(n\pi)^2 - \lambda}, \quad (43)$$

with $\lambda = c \ell^2$. The 2-loop amplitude $a_1 = -\beta^2 \langle W_4/4! \rangle$ consists of four diagrams depicted in Fig. 1, and those are respectively

$$\begin{aligned} (a) \quad & \lambda^2 \int_0^1 G(x)^2 = \frac{\lambda}{8} - \frac{3}{8} \sqrt{\lambda} X + \frac{3}{8} \lambda X^2, \\ (b) \quad & \lambda \int_0^1 G'(x)^2 = \frac{\lambda}{8} - \frac{1}{8} \sqrt{\lambda} X + \frac{1}{8} \lambda X^2, \\ (c) \quad & \lambda \int_0^1 G(x) G'''(x) = -\frac{\lambda}{8} - \frac{1}{8} \sqrt{\lambda} X + \frac{1}{8} \lambda X^2, \\ (d) \quad & \int_0^1 G''(x)^2 = \lambda^2 \int_0^1 G(x)^2, \end{aligned}$$

where $X = \cot \sqrt{\lambda}$, $G(x) = G(x, x')|_{x=x'}$, $G'(x) = (\partial/\partial x) G(x, x')|_{x=x'}$ and $G''(x) = (\partial^2/\partial x \partial x') G(x, x')|_{x=x'}$. While $G(x)$ and $G'(x)$ are convergent, $G''(x)$ diverges at the boundaries, thus we have found (c) and (d) by executing the x -integration first and then by regularizing

the infinite n -summation in terms of the following analytic continuations:

$$\begin{aligned} \sum_{n=1}^{\infty} \frac{1}{(n^2 + a^2)^s} &= -\frac{1}{2} a^{-2s} + \frac{\pi^{\frac{1}{2}}}{2} \frac{\Gamma(s - \frac{1}{2})}{\Gamma(s)} a^{-2s+1} \\ &+ 2 \frac{\pi^{\frac{1}{2}}}{\Gamma(s)} \sum_{n=1}^{\infty} \left(\frac{\pi n}{a}\right)^{s-\frac{1}{2}} K_{s-\frac{1}{2}}(2\pi n a), \end{aligned} \quad (44)$$

$$\begin{aligned} \sum_{n=1}^{\infty} \frac{n^2}{(n^2 + a^2)^s} &= \frac{\pi^{\frac{1}{2}}}{4} \frac{\Gamma(s - \frac{3}{2})}{\Gamma(s)} a^{-2s+3} \\ &+ \frac{\pi^{\frac{1}{2}}}{\Gamma(s)} \sum_{n=1}^{\infty} \left(\frac{\pi n}{a}\right)^{s-\frac{3}{2}} K_{s-\frac{3}{2}}(2\pi n a) \\ &- 2 \frac{\pi^{\frac{5}{2}}}{\Gamma(s)} \sum_{n=1}^{\infty} n^2 \left(\frac{\pi n}{a}\right)^{s-\frac{5}{2}} K_{s-\frac{5}{2}}(2\pi n a), \end{aligned} \quad (45)$$

$$\begin{aligned} \sum_{n=1}^{\infty} \frac{n^4}{(n^2 + a^2)^s} &= -\frac{3}{8} \pi^{\frac{1}{2}} \frac{\Gamma(s - \frac{5}{2})}{\Gamma(s)} a^{-s+\frac{5}{2}} \\ &+ \frac{3}{2} \frac{\pi^{\frac{1}{2}}}{\Gamma(s)} \sum_{n=1}^{\infty} \left(\frac{\pi n}{a}\right)^{s-\frac{5}{2}} K_{s-\frac{5}{2}}(2\pi n a) \\ &- 6 \frac{\pi^{\frac{5}{2}}}{\Gamma(s)} \sum_{n=1}^{\infty} n^2 \left(\frac{\pi n}{a}\right)^{s-\frac{7}{2}} K_{s-\frac{7}{2}}(2\pi n a) \\ &+ 2 \frac{\pi^{\frac{9}{2}}}{\Gamma(s)} \sum_{n=1}^{\infty} n^4 \left(\frac{\pi n}{a}\right)^{s-\frac{9}{2}} K_{s-\frac{9}{2}}(2\pi n a), \end{aligned} \quad (46)$$

where $K_\nu(z)$ is the modified Bessel function. Multiplying (a) through (d) with the weights of the diagrams, we conclude that the 2-loop amplitude vanishes. Beyond the 2-loop, however, we ought to generalize the analytic continuation for a multiple infinite summation. One might think that applying the analytic continuation method directly to the Green function, we could regularize the Green function, and thereby making all loop amplitude finite. This is certainly true, but regularizing the Green function in this way, we also eliminate the necessarily singularity at $x = x'$, and obtain non-vanishing 2-loop amplitude as a result. We may avoid this difficulty by treating $G(x, x')$ as a distribution w.r.t. x . Let us first examine this on the 2-loop and check if the amplitude vanishes. Since $G(x, x')$ may naturally be extended periodically (period 2) to \mathbb{R} as a function of x , one can redefine it as a distribution $\tilde{G}(x, x')$ such that

$$\begin{aligned} \tilde{G}(x, x') &= -\frac{1}{\sqrt{\lambda} \sin \sqrt{\lambda}} \sum_{n \in \mathbb{Z}} \left\{ \sin[\sqrt{\lambda}(x - 2n)] \sin[\sqrt{\lambda}(x' - 1)] H(x; 2n, x' + 2n) \right. \\ &\quad \left. + \sin[\sqrt{\lambda}x'] \sin[\sqrt{\lambda}(x - 2n - 1)] H(x; x' + 2n, 2n + 1) \right\} \\ &+ \frac{1}{\sqrt{\lambda} \sin \sqrt{\lambda}} \sum_{n \in \mathbb{Z}} \{x \rightarrow -x\}, \end{aligned} \quad (47)$$

where $H(x; a, b)$ denotes the characteristic function for the interval $[a, b] \subset \mathbb{R}$. Similarly $\tilde{G}(x)$ may also be extended periodically (period 1) to \mathbb{R}

$$\tilde{G}(x) = -\frac{1}{\sqrt{\lambda} \sin \sqrt{\lambda}} \sum_{n \in \mathbb{Z}} \left\{ \sin[\sqrt{\lambda}(x-n)] \sin[\sqrt{\lambda}(x-n-1)] H(x; n, n+1) \right\}. \quad (48)$$

Using the periodic delta function $\delta(x; n)$ (n is the period), we may evaluate the second derivative

$$\begin{aligned} \frac{\partial^2}{\partial x \partial x'} \tilde{G}(x, x') &= -\frac{\sqrt{\lambda}}{\sin \sqrt{\lambda}} \sum_{n \in \mathbb{Z}} \left\{ \cos[\sqrt{\lambda}(x-2n)] \cos[\sqrt{\lambda}(x'-1)] H(x; 2n, x'+2n) \right. \\ &\quad \left. + \cos[\sqrt{\lambda}x'] \cos[\sqrt{\lambda}(x-2n-1)] H(x; x'+2n, 2n+1) \right\} \\ &\quad - \frac{\sqrt{\lambda}}{\sin \sqrt{\lambda}} \sum_{n \in \mathbb{Z}} \{x \rightarrow -x\} + \delta(x-x'; 2) + \delta(x+x'; 2), \end{aligned} \quad (49)$$

and similarly

$$\tilde{G}''(x) = -\lambda \tilde{G}(x) - \sqrt{\lambda} \cot \sqrt{\lambda} + \frac{1}{2} \delta(x; 1). \quad (50)$$

The delta function appears only in $\tilde{G}''(x)$, and we confirm the vanishing of the 2-loop amplitude by using

$$\int_0^1 dx \delta(x; 1)^2 = \delta(0; 1) = 0, \quad (51)$$

which is consistent with the ζ -function regularization because of $\delta(0; 1) = 1 + 2\zeta(-1)$.

The 3-loop amplitude $a_2 = \beta^3 \langle \beta(W_4/4!)^2/2 - W_6/6! \rangle$ consists of 30 diagrams depicted in Fig. 2. Evaluating them by means of (47), (48) and $\delta(0; 1) = 0$, we find that 29 diagrams contain no ambiguities due to the the integration formulae

$$\int_0^1 dx \int_0^x dy \delta(x; 1) \delta(y; 1) F(x, y) = \frac{1}{8} F(0, 0) + \frac{1}{4} F(1, 0) + \frac{1}{8} F(1, 1), \quad (52)$$

$$\begin{aligned} \int_0^1 dx \int_0^x dy [\delta(x-y; 2) + \delta(x+y; 2)] [\delta(x; 1) + \delta(y; 1)] F(x, y) \\ = \frac{1}{2} F(0, 0) + \frac{1}{2} F(1, 1), \end{aligned} \quad (53)$$

$$\int_0^1 dx \int_0^x dy [\delta(x-y; 2) + \delta(x+y; 2)]^2 F(x, y) = \frac{1}{8} F(0, 0) + \frac{1}{8} F(1, 1). \quad (54)$$

Here the last equality follows from $\delta(0; 2) = 0$. Yet, in the diagram whose weight is -480 , we encounter an ambiguous integral

$$\int_0^1 dx \int_0^x dy [\delta(x-y; 2) + \delta(x+y; 2)] \delta(x; 1) F(x, y) = p F(0, 0) + q F(1, 1), \quad (55)$$

where $p + q = 1/2$ as is shown in (53), but p or q alone cannot be determined unless we specify the regularization of the delta function. If we were able to define the analytic continuation of the infinite double sum, this ambiguity would not appear, but we have no choice at our hand other than putting $q = 1/16$, and obtain the vanishing 3-loop amplitude as a result.

Ambiguities appearing in higher loops are inevitable, because they relate to the regularization ambiguity of the integration measure $\mathcal{D}\gamma$, which has never been defined rigorously in the first place. Both methods we have presented here reveal that the degree of ambiguity gets larger as the order of loops increases. In the analytic continuation method, ambiguity arises from the variety of the analytic continuation applicable to the multiple infinite summation, whereas in the distribution method, the delta-function integration, particularly the finite part of the boundary contribution, is the source of the ambiguity. Nevertheless our lower order calculations suggest that by regularizing $\mathcal{D}\gamma$ order by order, one can eliminate all higher loop corrections, and thereby preserving the Duistermaat-Heckman formula. The symplectic structure has been studied thoroughly in compact finite dimensional manifolds, but little is known for the infinite dimensional ones, which include most of the integrable hierarchies. This is exactly the place where the physical interests are, and the Duistermaat-Heckman formula would throw a new light over the integrable hierarchies as we have caught a glimpse of it here.

The authors would like to thank Dr. N. Sasaki for helpful discussions.

References

- [1] L.S. Da Rois, Rend. Circ. Mat. Palermo 22 (1906) 117.
- [2] F.R. Hama, Fluid Dynamics Res. 3 (1988) 149.
- [3] H. Hasimoto, J. Phys. Soc. Jap. 31 (1971) 293; J. Fluid Mech. 51 (1972) 477.
- [4] J. Madson and A. Weinstein, Physica 7D (1983) 305.
- [5] J. Langer and R. Perline, J. Nonlinear. Sci. 1 (1991) 71.
- [6] J.J. Duistermaat and G.J. Heckman, Inv. Math. 69 (1982) 259; *ibid.* 72 (1983) 153.
- [7] J.-L. Brylinski, Loop space, characteristic classes and geometric quantization, Prog. in Math. 111 (Birkhäuser, Berlin, 1993).
- [8] N. Koiso, Vortex filament equation and semilinear Schrödinger equation, Osaka Univ. preprint 1995.
- [9] N. Sasaki, *in preparation*.
- [10] L.D. Faddeev and L.A. Takhtajan, Hamiltonian methods in the theory of solitons, (Springer, Berlin, 1987).

- [11] M. Audin, The topology of torus action on symplectic manifolds, Prog. in Math. 93 (Birkhäuser, Berlin, 1994).
- [12] R.F. Picken, J. Phys. A: Math. Gen. 22 (1989) 2285.
- [13] E. Witten, J. Diff. Geom. 9 (1992) 303.
- [14] E. Keski-Bakkuri, A.J. Niemi, G. Semenoff and O. Tirkkonen, Phys. Rev. 44 (1991) 3899; A.J. Niemi and O. Tirkkonen, Ann. Phys. 235 (1994) 318; A.J. Niemi and K. Palo, Equivariant Morse theory and quantum integrability, hep-th/9406068.
- [15] H.M. Dykstra, J.D. Lykken and E.J. Raiten, Phys. Lett. B302 (1993) 223.
- [16] J. Riordan, Ann. of Math. Stat. 20 (1949) 419.
- [17] D.H. Adams and S. Sen, Phase and scaling properties of determinants arising in topological field theories, hep-th/9506079.

Figure captions

Figure 1. 2-loop diagrams. “Dot” denotes a derivative on the Green function; for instance, the propagator with one dot represents $G'(x)$, and the one with two dots $G''(x)$. The attached numbers are the weights of the diagrams.

Figure 2. 3-loop diagrams. Since there appear no second derivatives in (35) and the number of derivatives is always even, double dots on a single propagator must go to the separate vertices and the number of the derivatives at each vertex must be even. One must interpret dots accordingly for the diagrams with two vertices. Note that for a couple of diagrams in the top group and for a couple in the middle, though the resulting diagrams are inequivalent, this simple rule does not tell to which vertex dots are supposed to go. In those diagrams, dots are placed closer to the vertices to which they are supposed to go.

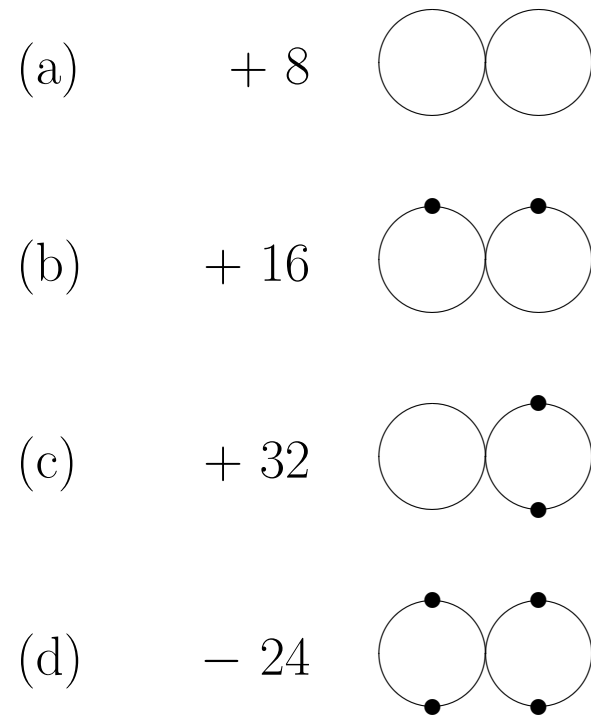


Figure 1

